

Sinusoidal phase grating created by a tunably buckled surface

Christopher Harrison,^{a)} Christopher M. Stafford, Wenhua Zhang, and Alamgir Karim
Polymers Division, National Institute of Standards and Technology, 100 Bureau Drive, Gaithersburg, Maryland 20899

(Received 7 June 2004; accepted 2 September 2004)

We investigate a buckling instability by both small angle light scattering and atomic force microscopy, demonstrating that a tunable phase grating can be created with a mechanical instability. The instability is realized in a prestressed silicone sheet coated with a glassy polymer film. Compression of the sample results in a sinusoidally wrinkled surface where the amplitude is controlled by the degree of compression and the wavelength by film thickness. We model the system with Fourier optics, explaining the positions and relative intensities of the diffraction orders. [DOI: 10.1063/1.1809281]

The phenomenon of buckling is typically associated with a catastrophic failure, such as with the collapse of a column or bridge.¹ Here, we will investigate a less dramatic mode of failure with a sinusoidally buckled surface of a multilayer sandwich panel and demonstrate its utility as a tunable phase grating.^{2,3} By merely controlling the amplitude of the buckles, we are able to tune the intensity of the diffraction orders of a scattered laser beam by more than three orders of magnitude. This wrinkling phenomenon, previously observed in an analogous system by Bowden and co-workers, has recently attracted great attention as a measurement technique due to its sensitivity to the mechanical properties of thin films.^{4–6}

Samples were prepared by first casting polydimethylsiloxane [(PDMS), Dow Corning Sylgard 184] sheets (3 mm thick) at a base to catalyst mixing ratio of 20:1 by weight.⁷ The mixture was allowed to degas overnight and then baked for 1 h at 60 °C in a forced-air oven. Coupons (50 mm by 75 mm) were clamped onto a strain stage and prestressed by elongating 30%.⁸ The index of refraction of PDMS was measured to be 1.404 ± 0.004 at the wavelength $\lambda = 632$ nm by determining the Brewster angle. The modulus of the silicone coupons was measured with a Texture Analyzer (TA-XT2i). A 3 in. silicon wafer was treated with ultraviolet light and ozone (Jelight 342) to make the surface hydrophilic. Atactic polystyrene [(PS), Aldrich, $M_w = 2.80 \times 10^5$, $M_w/M_n = 3.07$] films were spincoated from toluene at a thickness of $218 \text{ nm} \pm 2 \text{ nm}$ as measured by a Filmetrics F-20 interferometer.⁹ A centimeter-sized wafer piece was cleaved from the spin-coated wafer and placed onto the stretched silicone coupon with the film side down. The strain stage was immersed under water, releasing the film and transferring it to the PDMS with little or no residual stress. The tackiness of the PDMS assures perfect adhesion of the PS film.

Figure 1 shows a series of tapping mode atomic force microscopy (AFM) micrographs (Digital Instruments, Dimension Model 3100) that illustrate the increase of buckling amplitude w with compressional strain Δ . Throughout this letter, strain will refer to the degree of compression of the polymer film, not the prestressed silicone coupon. The relaxed film at zero strain [Fig. 1(a)] is smooth and exhibits no

periodic topography. At a compressional strain of approximately 0.010 (typical strain uncertainty was 0.001), the sample abruptly buckles with a wrinkling amplitude w of $0.08 \mu\text{m}$ [Fig. 1(b)].¹⁰ The buckling wavelength d arises from the buckling instability and can be calculated as:^{11,12}

$$d = \alpha h \left[\frac{E_p}{E_m} \right]^{1/3}, \quad (1)$$

where h is the film thickness, E_p and E_m are the instantaneous moduli of the film and silicone, respectively, and α is a unit-less prefactor equal to $2\pi[(3 - \nu_m)(1 + \nu_m)/12]^{1/3}$.⁶ For silicone with a Poisson ratio ν_m of 0.5 and modulus of 0.5 MPa, a film of modulus 3.2 GPa and of thickness 218 nm, we calculate a wavelength of $17.2 \mu\text{m}$, in good agreement with the measured wavelength d of $18.1 \mu\text{m}$ [Figs. 1(b)–1(d)].

In contrast to the mechanically determined wavelength, the amplitude w of the periodically wrinkled surface can be reversibly tuned by the degree of compression, satisfying the

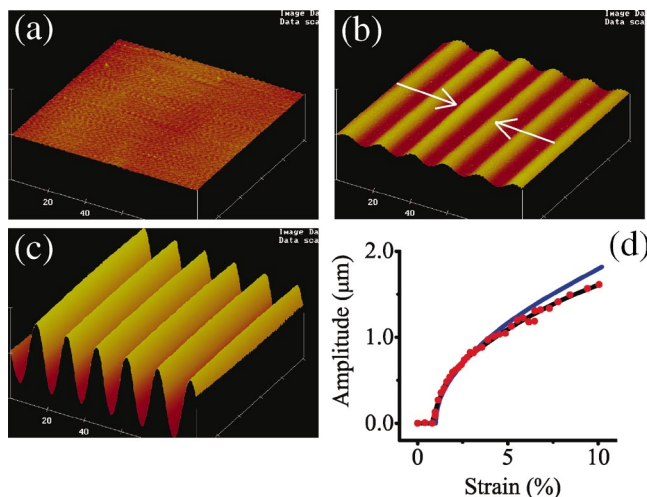


FIG. 1. (Color) (a)–(c) AFM micrographs ($100 \times 100 \mu\text{m}$) of PS-coated silicone sheet as a function of strain. (a) At zero strain, the surface is flat. (b) At a strain of 0.010 (arrows show compression direction), the surface abruptly wrinkles with an amplitude and wavelength of 0.08 and $18.1 \mu\text{m}$, respectively. (c) At a strain of 0.073, the amplitude has nonlinearly increased to $1.37 \mu\text{m}$. (d) Amplitude w vs strain Δ as measured from AFM images [data indicated by red circles, fit $w(\Delta)$ in black]. Amplitude calculated from model is shown in blue. The experimental uncertainty, taken as one standard deviation, is comparable to symbol size.

^{a)}Current address: Sensor Physics Department, Schlumberger-Doll Research, 36 Old Quarry Road, Ridgefield, CT 06877.

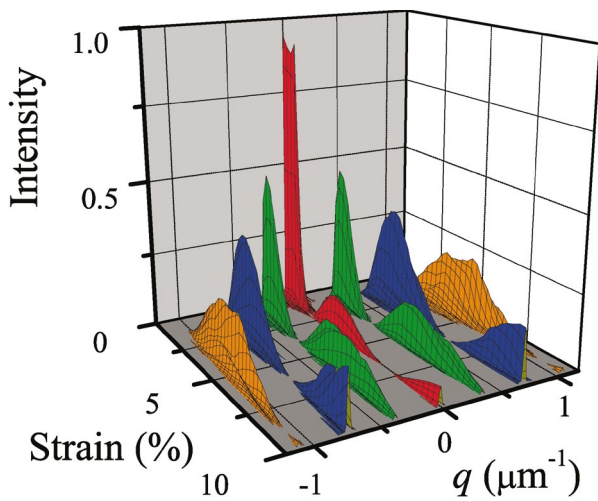


FIG. 2. (Color) Normalized SALS (I/I_0) data as a function of strain Δ . The zeroth, first, second, and third orders (red, green, blue, and orange, respectively) can be seen to cycle through maxima and minima as the strain (hence, amplitude w) increases.

constraint that the length of the PS film is fixed. Algorithms were developed to measure both the wavelength d and amplitude w of such AFM micrographs, the latter of which is plotted in red in Fig. 1(d). The amplitude can be seen to grow nonlinearly with strain, increasing to $1.6 \mu\text{m}$ at a strain of 0.10. The wavelength d decreased by only 9% over the same range of strain. From these data, we generated a smoothly increasing function [$w(\Delta)$, shown in black] which we will use to convert the compressional strain to a wrinkling amplitude for small angle light scattering (SALS) studies shown in Fig. 3. Modeling the film as a line of fixed contour length and constrained wavelength reveals an amplitude that increases faster with strain than our measured data [blue line in Fig. 1(d)]. The discrepancy at higher strains is consistent with a slightly decreasing in wavelength (not accounted for in our model), which may result from a strain-dependent PDMS modulus.

SALS was performed on identically prepared samples in transmission mode with a conventional HeNe laser and a Roper Scientific charge coupled device (CCD) camera (RTE/CCD-1300-Y/HS). A planoconvex converging lens with a 50 cm focal length brought the diffraction pattern into the Fraunhofer limit within the dimensions of an optical table. The laser was oriented normal to the sample surface and passed first through a rectangular aperture. Samples were oriented such that the line of diffraction peaks were aligned along the \hat{q}_x direction. Though the topography of the sinusoidally wrinkled surface can be well described by a single spatial frequency (Fig. 1), the phase shift imparted by this surface produces diffraction orders at all harmonics. The intensities of these harmonics depend upon the wrinkling amplitude, which depends upon the sample strain [Fig. 1(d)]. For each degree of compressional strain Δ , a slice of the diffraction pattern was extracted with an extent in the \hat{q}_y direction which was smaller than the characteristic spot size. We have color coded the orders and constructed a surface where \hat{q}_x has been replaced with wavenumber q in Fig. 2. As the sample is compressed (increasing strain), the wrinkling amplitude increases and causes the diffraction orders to cycle through maxima and minima.¹⁰ For example, the zeroth or-

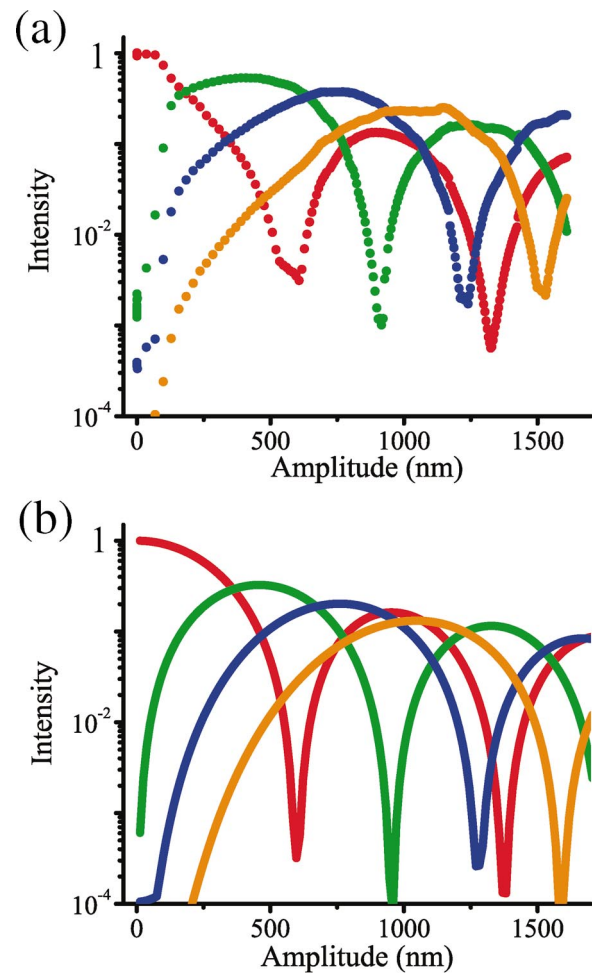


FIG. 3. (Color) (a) Normalized intensities of the zeroth-, first-, second-, and third-order diffraction peaks (plotted in red, green, blue, and orange, respectively) as a function of wrinkling amplitude. Each order exhibits at least one minima. The zeroth order has decreased by three orders of magnitude at its point of minimum intensity ($w=1330 \text{ nm}$). (b) Modeled diffraction pattern showing good agreement with data.

der (red) exhibits two minima and the remaining orders each exhibit at least one minimum as well.

As coherent light passes through a wrinkled surface, a local phase shift is imparted with a magnitude proportional to the wrinkling amplitude. The diffraction pattern from a coherent beam normal to a transparent surface with a sinusoidal topography can be calculated, in the Fraunhofer limit,² as:

$$I[q] \approx \sum_{p=-\infty}^{\infty} J_p^2\left(\frac{m}{2}\right) \text{sinc}^2\left[\frac{W}{\pi}\left(q - \frac{2p\pi}{d}\right)\right], \quad (2)$$

where J_p is the Bessel function of the first kind, W is the half-width of the aperture in the \hat{x} direction, d is the wrinkling wavelength again, $m/2$ is the maximum phase shift imparted to the light, and p is an index. Since the sinc function is narrowly distributed in q about each order without significant overlap between adjacent orders, the maximum intensity of the p th order is simply proportional to the Bessel function $J_p^2(m/2)$. As $m(\Delta)$ is a monotonic function of strain, each color-coded diffraction order in Fig. 2 adopts an only slightly distorted form of the associated Bessel function. We transform $m(\Delta)$ to $w(\Delta)$ by the following relation:

$$\frac{m(\Delta)}{2} = 2\pi \frac{w(\Delta)}{\lambda} [n - 1], \quad (3)$$

where Δ is the compressive strain, n is the index of refraction of the silicone, λ is the laser wavelength, and $w(\Delta)$ is determined from Fig. 1. In this approximation, we do not include the additional phase shift imparted by the PS film ($n=1.59$) which is valid as long as $w/d \ll 1$. After transformation, a satisfying comparison can be made between measurement [Fig. 3(a)] and model [Fig. 3(b)] by focusing on the maximum diffraction intensities of the zeroth- through third-order peaks as a function of surface wrinkling amplitude. We plot the intensities of these orders in Fig. 3(a) as a function of wrinkling amplitude by transforming each strain in Fig. 2 to an amplitude using $w(\Delta)$. The intensity of the orders can be seen to pass through maxima and minima as in Fig. 2. There is good agreement between data and our modeling, including the locations of the minima as well as the magnitude of the relative intensities of the maxima. For example, the minima of the zeroth and first orders, occurring at wrinkling amplitudes of 580 nm and 905 nm, respectively, are in good agreement with their calculated minima of 600 nm and 946 nm. The relative intensities of the maxima of the diffraction orders are generally in good agreement with the model as well, though the first maximum of the zeroth order appears to be weaker than the calculation, possibility due to scattering from impurities.¹⁰

In summary, we have shown that a relatively rigid film coated onto a silicone sheet can act as a tunable phase grating. The intensity of the diffraction peaks can be tuned by three orders of magnitude. This process may have applicability as an inexpensive technique to tune a coherent beam's intensity.

Two of the authors (CMS and CH) acknowledge the National Research Council Postdoctoral Fellowship Program. The authors thank Thomas A. Germer for measurement of the index of refraction. They cheerfully acknowledge useful conversations with Jack F. Douglas, Ronald L. Jones, Steve D. Hudson, and Jan Groenewold. This manuscript is an official contribution of the National Institute of Standards and Technology; not subject to copyright in the United States.

¹S. P. Timoshenko and S. Woinowsky-Krieger, *Theory of Plates and Shells* (McGraw-Hill, New York, 1959).

²J. W. Goodman, *Introduction to Fourier Optics*, 2nd ed. (McGraw-Hill, New York, 1996).

³J. E. Harvey (unpublished).

⁴N. Bowden, S. Brittain, A. G. Evans, J. W. Hutchinson, and G. M. Whitesides, *Nature (London)* **383**, 146 (1998).

⁵E. Cerda, K. Ravi-Chandar, and L. Mahadevan, *Nature (London)* **419**, 579 (2002).

⁶C. M. Stafford, C. Harrison, K. L. Beers, A. Karim, E. J. Amis, M. R. VanLandingham, H.-C. Kim, W. Volksen, R. D. Miller, E. E. Simonyi, *Nat. Mater.* **3**, 545 (2004).

⁷Equipment and instruments or materials are identified in the paper in order to adequately specify the experimental details. Such identification does not imply recommendation by NIST, nor does it imply the materials are necessarily the best available for the purpose.

⁸C. M. Stafford and C. Harrison, "SIEBIMM: Strain-Induced Elastomer Buckling Instability for Mechanical Measurements, Instrumentation Document," which can be obtained via www.nist.gov/combi or by email at combi@nist.gov

⁹According to ISO 31-8, the term "molecular weight" has been replaced by "relative molecular mass," M_r . The conventional notation, rather than the ISO notation, has been employed for this publication.

¹⁰The silicone used here typically contains 30% silica particles (J. Genzer, private communication) which cause distortions in the stress field, scattered light, and altered the measured intensity. This also causes a small amount of amplitude nonuniformity near silica flocculates at the onset of buckling.

¹¹H. G. Allen, *Analysis and Design of Structural Sandwich Panels* (Pergamon, New York, 1969).

¹²J. Groenewold, *Physica A* **298**, 32 (2001).